

Automated Federated Pipeline for Parameter-Efficient Fine-Tuning of Large Language Models

Zihan Fang, Zheng Lin, Zhe Chen *Member, IEEE*, Xianhao Chen, *Member, IEEE*,
Yue Gao *Fellow, IEEE*, and Yuguang Fang *Fellow, IEEE*

Abstract—Recently, there has been a surge in the development of advanced intelligent generative content (AIGC), especially large language models (LLMs). For many downstream tasks, it is necessary to fine-tune LLMs using private data. While federated learning offers a promising privacy-preserving solution to LLM fine-tuning, the substantial size of an LLM, combined with high computational and communication demands, makes it hard to apply to handle downstream tasks. More importantly, private edge servers often possess varying computing and network resources in real-world scenarios, introducing additional complexities to LLM fine-tuning. To tackle these problems, we design and implement an automated federated pipeline, named FedPipe, to fine-tune LLMs on heterogeneous edge servers with minimal training cost and no additional inference latency. FedPipe firstly identifies the weights to be fine-tuned based on their contributions to the LLM training. It then configures a low-rank adapter for each selected weight within the resource constraints of the edge server and aggregates these local adapters from all edge servers to fine-tune the whole LLM. Finally, it appropriately quantizes the parameters of LLM to reduce memory space according to the requirements of edge servers. Extensive experiments demonstrate that FedPipe expedites model training and achieves higher accuracy than the state-of-the-art benchmarks.

Index Terms—federated learning, large-scale language model, fine-tuning.

I. INTRODUCTION

We are now witnessing the tremendous success of advanced intelligent generative content (AIGC) [1], especially large language models (LLMs), such as OpenGPT [2], [3], LLaMa [4], and Palm [5], in our daily life. Due to the huge number of model parameters (e.g., OpenGPT3 has 175 B parameters), those LLMs deliver outstanding performance on various natural language processing (NLP) applications, especially, questions and answers [6]–[8], sentiment analysis [9], [10], etc. It is believed that many new exciting applications will come out in the near future such as smart healthcare, intelligent transportation, and image classification [11]–[16].

Z. Fang, Z. Chen and Y. Gao are with the School of Computer Science, Fudan University, Shanghai 200438, China (e-mail: zhechen@fudan.edu.cn; gao_yue@fudan.edu.cn). Z. Fang is also with the Department of Computer Science, City University of Hong Kong, Kowloon, Hong Kong SAR, China (e-mail: zihanfang3@cityu.edu.hk).

Z. Lin and X. Chen are with the Department of Electrical and Electronic Engineering, University of Hong Kong, Pok Fu Lam, Hong Kong, China (e-mail: linzheng@eee.hku.hk; xchen@eee.hku.hk).

Yuguang Fang is with the Department of Computer Science, City University of Hong Kong, Kowloon, Hong Kong SAR, China (e-mail: my.fang@cityu.edu.hk).

(Corresponding author: Yue Gao)

Considering the state-of-the-art workflow of LLMs, generally, we can summarize into three phases: 1) pre-training LLMs from scratch with extensive computing resources (e.g., training GPT3-1.3B model requires 64 Tesla V100 GPUs for one week [17]) and tremendous text corpora (e.g., Wikipedia); 2) fine-tuning pre-trained LLMs for various downstream tasks; and 3) deploying fine-tuned LLMs at an edge server to infer from input data.

Due to privacy concerns, even if many parties with the same downstream task demand a shared LLM, they cannot directly contribute their raw data to fine-tune it [18]–[21]. For example, several hospitals would like to fine-tune an LLM for a special disease diagnosis via their edge servers [22], [23], but they cannot share their patients' data. Although federated learning (FL) is a promising solution to address this privacy issue [24]–[29], it is non-trivial to fine-tune LLMs via FL due to the limited computing capability of edge servers. In typical configurations, edge servers are outfitted with low-cost, commercially available GPUs, such as the NVIDIA GeForce RTX 3090-Ti. These GPUs, while powerful for many applications, are outmatched by the more robust GPUs found in data center environments [30], [31]. Specifically, data centers often deploy data-center-grade GPUs like the NVIDIA A100 and V100, characterized by significantly higher communication bandwidth (e.g., NVLink), larger graphic memory, and enhanced computing capabilities. This distinction in hardware resources has critical implications for computational tasks [32]–[34], notably, edge servers face challenges in supporting full parameter fine-tuning of LLMs within standard FL frameworks.

Fortunately, the integration of FL and Parameter-Efficient Fine-Tuning (PEFT) may solve the above challenges. Recent research efforts [35]–[42] have explored PEFT methods, in particular, *ADAPTER* [35], [36], [38] and *LoRA* [37], [42], to mitigate the challenges of intensive computational resources required by LLM fine-tuning. Fig. 1 illustrates how to integrate PEFT with FL for LLMs. The central server distributes a pre-trained LLM to edge servers (participants), and then edge servers perform local training using PEFT methods. After training, the central server aggregates these updates and redistributes the enhanced LLM to edge servers for subsequent training rounds. This iteration continues until the LLM achieves a predefined accuracy threshold. Recent work, *FedAdapter* [43], adopts *ADAPTER* to achieve efficient FL for NLP downstream fine-tuning, but mainly focuses on standard language model, such as BERT [44]. A few research

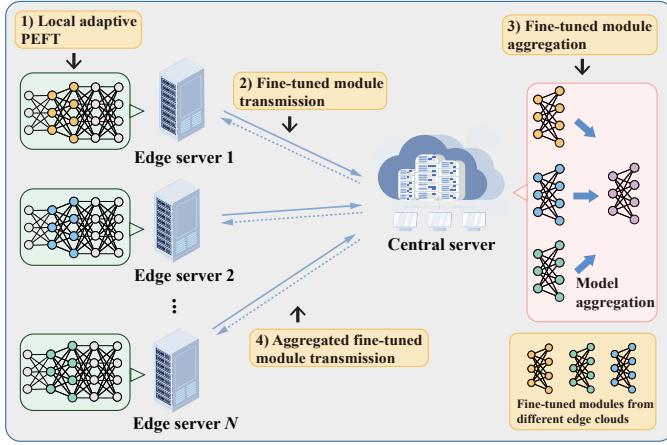


Fig. 1: A scenario of LLM FL via PEFT with edge servers.

works [45], [46] study LLM FL with PEFT, but they always assume every edge server with homogeneous resources (i.e., computing power and memory). Consequently, these frameworks are not well adapted to heterogeneous environments and cause deterioration in training performance. In practice, it is still non-trivial to integrate PEFT with FL in LLMs for downstream tasks.

In this paper, we propose and implement an automated federated pipeline (FedPipe) for LLM FL fine-tuning. Unlike existing PEFT methods, FedPipe does not aim to introduce new PEFT techniques. Instead, it serves as a foundational framework to enhance any existing PEFT method. This is achieved by systematically decoupling, abstracting, and automating the operations and parameters of these methods. As a result, application and algorithm developers can efficiently outsource the implementation intricacies of LLM FL fine-tuning, allowing them to concentrate on their main services or model design. Despite the promising potential of FedPipe, how to implement this framework poses significant challenges. First, given the varying computing resources across edge servers, this heterogeneity causes a pronounced straggler problem in FL [47]–[52]. For instance, two edge servers with slightly different GPU memories (e.g., 22GB vs. 24GB) can experience a training time discrepancy of several hours per communication round in FL. Second, to offer better fine-tuning performance, FedPipe enables each edge server to identify and prioritize important weights for adapter construction. However, assessing and modeling the importance of these weights remains an open problem. Finally, each adapter within FedPipe must align well with the computing budget of its respective edge server, which demands careful adjustment of model parameters. These challenges underscore the complexity and necessity of careful design of FedPipe.

In this paper, we first conduct pilot measurements to analyze the above challenges and acquire the corresponding insights to guide the system design of FedPipe. Then, we formulate the automated LLM FL fine-tuning pipeline as a Mixed-Integer Linear Programming (MILP) optimization problem. To solve the MILP problem, we propose a two-stage method, comprised of trainable weights identification method and fast search algorithm. The adaptive identification method of important

weights is used to figure out the best adapter of an LLM to fine-tune based on their importance score for each edge server. This method parameterizes incremental updates (i.e., trainable weights) using singular value decomposition (SVD) to effectively prune unimportant updates with the lower singular values, leading to the efficient adapter with fewer trainable weights. According to the adapters of edge servers, by considering heterogeneous computing resources of edge servers, we design a fast search algorithm to select the best set of rank and batch size for local training at each edge server. Finally, to consider diverse memory budgets for edge servers, and further accelerate their training speed, we leverage a simple quantization-agnostic backward pass to adaptively achieve low-precision LLM weights from a customized black-box quantization module. Moreover, different from existing LLM FL aggregation approaches, we design a lightweight partial weights aggregation approach by only aggregating local adapters to improve communication efficiency.

We summarize our main contributions of FedPipe as follows.

- FedPipe is the first general automated federated pipeline of fine-tuning LLMs for all kinds of downstream tasks.
- We formulate the pipeline as an MILP optimization problem and develop an efficient algorithm to solve it.
- By taking heterogeneous computing resources at edge servers into consideration, we develop an effective method to find different low-rank adapter structures for heterogeneous edge servers.
- To further reduce the computational complexity in solving our MILP at edge servers, we also design a fast search algorithm to dynamically identify important parameters for local adapter training.
- Furthermore, according to those parameters and memory budgets of edge servers, we quantize the local models into different quantization bits to increase training efficiency.
- We design a partial weight aggregation approach to aggregate all adapters without increasing communication overhead.

The rest of this paper is organized as follows. Section II introduces the background and motivation and the system design of FedPipe is presented in Section III. Sections IV and V respectively elaborate FedPipe’s implementation and report the extensive evaluations of FedPipe. Section VI briefly discusses the related works, followed by the conclusion in Section VII.

II. BACKGROUND AND MOTIVATION

Before we delve into detailed design analysis and details, we briefly introduce the background of PEFT for LLM FL. Then, to better motivate the design of FedPipe, we provide extensive pilot measurement studies to elaborate the design challenges of FL on LLMs.

A. Injecting PEFT into Federated Learning on LLMs

Due to the constrained computing resources at an edge server (i.e., commercial GPUs, such as NVIDIA GeForce RTX 3090-Ti) and the large number of parameters in an LLM, full parameter fine-tuning (i.e., initializing the model with

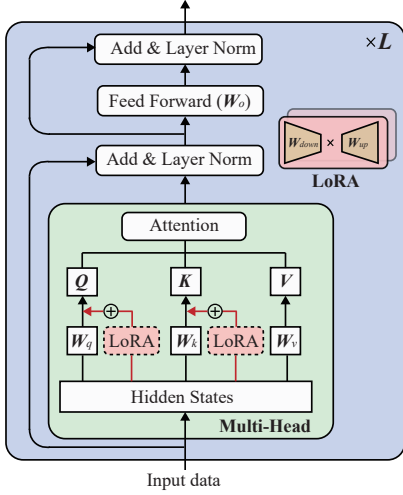


Fig. 2: An illustration of LoRA method.

pre-trained weights, updating all parameters, and generating separate instances for various tasks) at each edge server leads to unacceptable computing and networking latency in both model training and aggregation. Table I illustrates the number of parameters and sizes of several popular LLMs. Obviously, the smallest model, GPT-2 [2] with 774M parameters, is over 7 times larger than the conventional language model (e.g., BERT [44]) with 110M parameters.

To combat the above stumbling obstacles in LLM FL, PEFT employed in downstream task training is a potential solution. Different from the full parameter fine-tuning, PEFT only fine-tunes parts of neurons to reduce trainable parameters in a model, leading to less computing cost. Recently, there are mainly two types of PEFT, ADAPTER [35], [36], [38] and LoRA [37], [42]. As shown in Fig. 2, ADAPTER inserts a few layers for each transformer block [35] and only trains those layers in a pre-trained model. Apparently, ADAPTER introduces extra latency in the inference phase, due to its additional layers [37]. However, LoRA is an adapter with low-rank adaptation without additional inference latency that injects trainable rank decomposition matrices into each transformer layer, but freezes all weights of a pre-trained model. Many works [37], [41], [42] have verified that LoRA outperforms ADAPTER, and hence in the following, we only focus on LoRA.

To better understand the computing and communication bottlenecks in the LLM FL, we set up two experiments using one of the most prevalent LLMs, GPT-2. Fig. 3a and 3b show the training time for a batch of data and exchanged parameters of full parameter fine-tuning and PEFT. Full parameter fine-tuning obtains more than 1.4 and 1000 times larger than those of PEFT in training and exchanging, respectively. Apparently,

Model	#Trainable Parameters	Size
BERT	110 M	0.44 GB
GPT-2	774 M	3 GB
GPT-3	175 B	700 GB
LLaMA-1	65 B	260 GB
LLaMA-2	70 B	280 GB

TABLE I: Popular LLMs

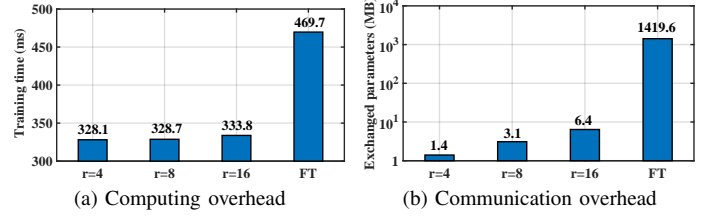
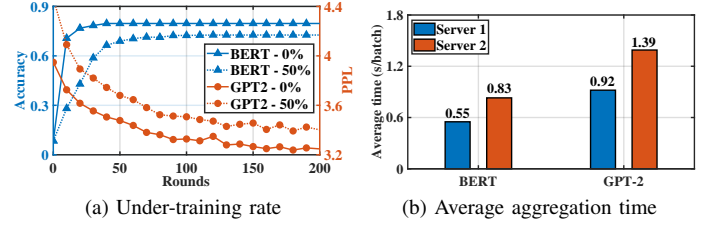
Fig. 3: The training time, and exchanged parameters of LoRA and full parameter fine-tuning for GPT-2, where r is the rank size of LoRA adapter.

Fig. 4: The straggler problem on GPT-2 and BERT.

instead of the entire model fine-tuning, PEFT can significantly mitigate computing and communication overhead. However, we also meet three main challenges to integrate PEFT into LLM FL. We will use “training” to represent fine-tuning in the following sections.

B. Severe Straggler Problem in LLM FL

State-of-the-art LLM FL frameworks [45], [46] usually assume that each edge server has sufficient local resources (e.g., computing power, communication bandwidth, and memory space) to perform local model training. Therefore, a central server can easily aggregate these local models to achieve good performance. However, in practice, the available resources of various edge servers vary significantly, and the allocated resources for training may change at run-time depending on how on-demand running programs prioritize resource allocation. More importantly, due to the large parameters of LLM, the resource heterogeneity of edge servers leads to significantly different training time, and a severe straggler problem in model aggregation.

To better understand the impact of heterogeneous resources on the straggler problem for LLM FL, we conduct two experiments for a standard model and LLM. We integrate LoRA into FedAvg [53], one of the most prevalent FL frameworks, to evaluate its performance on the widely recognized LLM GPT-2 and standard model BERT for homogeneous and heterogeneous cases. We set up two PC servers (i.e., edge servers) with/without varying computing power by controlling different graphic memories of GPU (22GB and 24GB), but the same ones (24GB) for homogeneous and heterogeneous cases, respectively. The result is shown in Fig. 4 where the under-training rate is defined to be the number of under-training edge servers divided by the total number of edge servers and the average aggregation time means the per-round time from the start of local model training for a batch of data to the end of model aggregation.

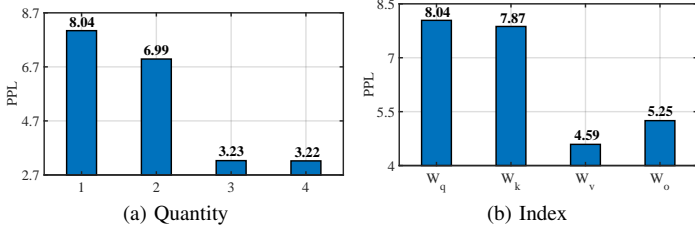


Fig. 5: GPT-2 training performance with different trainable weights, where the trainable weights combinations corresponding to quantities 1, 2, 3, and 4 are $\{W_q\}$, $\{W_q, W_k\}$, $\{W_q, W_k, W_v\}$, and $\{W_q, W_k, W_v, W_o\}$, respectively.

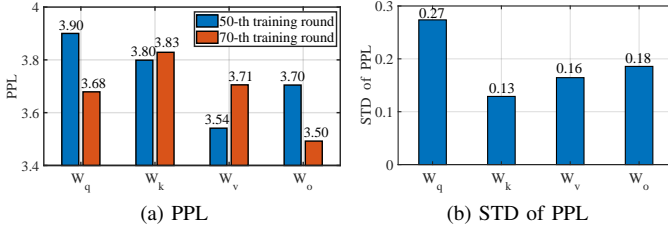


Fig. 6: The PPL at the 50-th and 70-th training rounds and the STDs of the PPL across 100 training rounds.

It is clear to see that the straggler problem occurs in the heterogeneous case for both the standard model and LLM. However, for the heterogeneous case, even if the difference in computing capabilities between two edge servers is 10 TFLOPS, LLM achieves much worse performance than standard one in both under-training rate and aggregation time. Therefore, we need to develop an efficient FL fine-tuning pipeline for LLMs to accommodate heterogeneous resources on different edge servers.

C. Weight-Level Configuration

Although LoRA has reduced large computing overhead (see Section II-A) for LLMs, due to the constrained computing capacity at an edge server, training all weights with LoRA in each layer still poses a heavy workload. We train multiple LoRA adapter versions by increasing the number of trainable weights in each layer shown in Fig. 5a. The perplexity (PPL) is used as the performance indicator to evaluate how well the model has learned the distribution of the data it was trained on, and a smaller PPL represents better performance. Apparently, the more weights the LoRA adapter has, the higher the computing overhead, and the better the performance required and obtained. A naive solution is to configure the number of trainable weights based on a computing budget.

However, how to find the prior weights is a non-trivial task. We have conducted another measurement experiment to study the impact of weight indices in LoRA training. We select four trainable weight vectors (i.e., W_q , W_k , W_v , W_o shown in Fig. 2) from the transformer block to train LoRA adapters in an round illustrated in Fig. 5b. It demonstrates that various weight indices have different performances. We also plot PLLs with four trainable weight vectors in different training rounds shown in Fig. 6a, and calculate their stan-

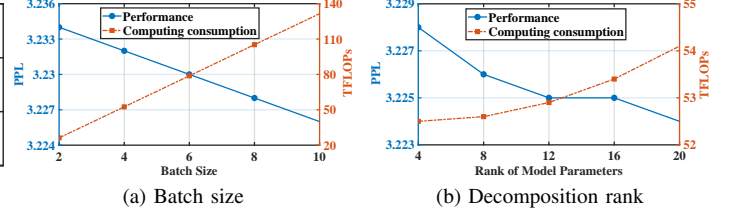


Fig. 7: Performance and computing consumption of GPT-2 with LoRA adapter with different training batch sizes and ranks.

dard deviations (STDs) illustrated in Fig. 6b. Apparently, the importance of four trainable weight vectors changes for the LoRA adapter in each training round, and hence, a one-shot measurement cannot identify their priority. Therefore, we need to investigate how to identify and prioritize the important trainable weights automatically for each edge server under its computing budget.

D. Budget-Aware Model Parameters Alignment

While the training weights are determined, several parameters still impact LoRA training, in particular, *batch size*, *decomposition rank*, *dropout*, *alpha*, etc. We evaluate all of them and find that batch size and decomposition rank are the two most important parameters for training performance¹. To study the impact of both batch size and decomposition rank, we increase them, respectively, to train the pre-trained GPT-2 with LoRA, and the results are illustrated in Fig. 7. It is clear to observe that a larger batch size or decomposition rank always offers better performance but consumes more computing resources. However, given the computing budget of an edge server, we cannot always select the largest batch size and rank. We need to find an optimal combination of batch size and rank under the computing budget for each edge server in an automated federated pipeline.

III. AUTOMATED FEDERATED PIPELINE DESIGN

A. Overview of FedPipe

To tackle the above challenges, we design FedPipe, an automated federated pipeline shown in Fig. 8, to determine the optimal fine-tuning model structure to improve the performance of fine-tuning LLMs, accommodating heterogeneous and resource-constrained edge servers. We first theoretically formulate an MILP to address the straggler problem under heterogeneous and constrained computing resources in LLM FL to guide FedPipe's design (Section III-B). To solve the problem, we propose two-level solutions to identify the important weights (Section III-C) and heterogeneous adapters' configuration (Section III-D). We also consider heterogeneous storage memories and quantize the LLM based on the budget of an edge server (Section III-E). Finally, we design an effective method to aggregate all local models with different size of LoRA adapters (Section III-F). After that, the next training round starts.

¹The same results are also observed in [42], [54]

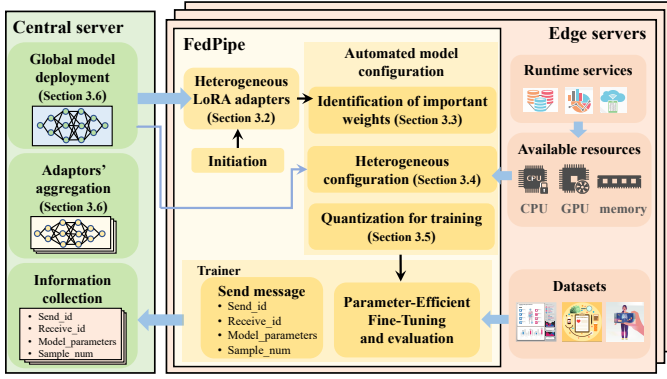


Fig. 8: The system overview of FedPipe.

B. Modelling Heterogeneous LoRA Adapters

In this section, we model the LoRA adapters for different edge servers with heterogeneous computing resources. As illustrated in Fig. 9, N edge servers independently train LoRA adapters, each with its computing budget $C_{i,max}$ for the i -th edge server. After training, the central server aggregates all LoRA adapters of edge servers. LoRA is built on the insights that over-parametrized models essentially reside on a low intrinsic dimension [55], and thus, can be characterized with the reduced number of trainable parameters. LoRA augments the parameters of the frozen pre-trained model with an additional factorized projection, which constrains weight updates by representing them with a low-rank decomposition $\mathbf{W} = \mathbf{W}_0 + \Delta\mathbf{W}$, where $\Delta\mathbf{W} = \mathbf{B}\mathbf{A}$, $\mathbf{B} \in \mathbf{R}^{d_i \times r}$ and $\mathbf{A} \in \mathbf{R}^{r \times d_o}$ denote the incremental matrix and rank decomposition matrices, respectively. The rank is $r \ll \min(d_i, d_o)$ (e.g., $r = 8$ when $d_i = d_o = 1024$), and the dimensions of input and output of rank decomposition matrices \mathbf{B} and \mathbf{A} are d_i and d_o , respectively. The LoRA adapter is the cascade structure composed of \mathbf{B} and \mathbf{A} .

The trainable weight of the i -th edge server is denoted by \mathbf{W}_i , and its local training dataset $\mathcal{D}_i = \{\mathbf{x}_{i,j}, y_{i,j}\}$, where $\mathbf{x}_{i,j}$ and $y_{i,j}$ represent the j -th input data and its corresponding label, respectively. Thus, the local loss function for the i -th edge server can be denoted as $L_i(\mathbf{W}_i) = \frac{1}{|\mathcal{D}_i|} \sum_{j=1}^{|\mathcal{D}_i|} L_{i,j}(\mathbf{x}_{i,j}, y_{i,j}; \mathbf{W}_i)$ where $L_{i,j}(\mathbf{x}_{i,j}, y_{i,j}; \mathbf{W}_i)$ represents the sample-wise loss function for the j -th data sample in the local dataset \mathcal{D}_i . Denote the total dataset as $\mathcal{D} = \bigcup_{i=1}^N \mathcal{D}_i$, the global loss function is expressed as the weighted average of the local loss functions. To find the optimal model parameters \mathbf{W}^* , the learning objective of the global model can be formulated as

$$\min_{\mathbf{W}} L(\mathbf{W}) = \min_{\mathbf{W}} \sum_{i=1}^N \frac{|\mathcal{D}_i|}{|\mathcal{D}|} L_i(\mathbf{W}) \quad (1)$$

$$\text{where } \mathbf{W} = \sum_{i=1}^N \frac{|\mathcal{D}_i|}{|\mathcal{D}|} \mathbf{W}_i.$$

Recalling Section II-C, batch size and rank affect the LoRA training performance directly, and thus, we rewrite Eqn. (1) in

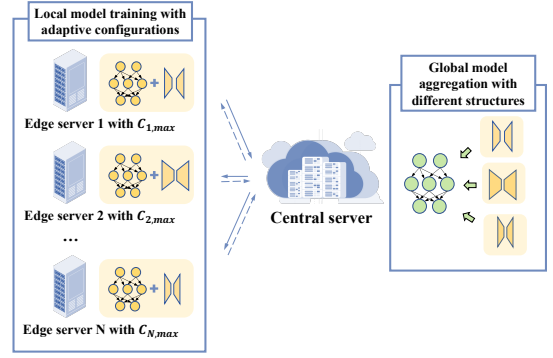


Fig. 9: Integrating LoRA adapters into LLM FL.

the following way

$$\min_{b_i, \mathcal{R}_i, \mathcal{W}_i} \sum_{i=1}^N \frac{|\mathcal{D}_i|}{|\mathcal{D}|} L_i(\mathbf{W}|b_i, \mathcal{R}_i, \mathcal{W}_i), \quad (2a)$$

$$\text{s.t. } b_{min} \leq b_i \leq b_{max}, \quad (2b)$$

$$\mathcal{W}_i \in \{\mathbf{W}_q, \mathbf{W}_k, \mathbf{W}_v, \mathbf{W}_o\}, \quad (2c)$$

$$r_i^m \in \mathcal{Q}^m, \quad (2d)$$

$$b_i \cdot f_c(\mathcal{W}_i, \mathcal{R}_i) \leq C_{i,max}, \quad (2e)$$

where \mathcal{W}_i and $\mathcal{R}_i = \{r_i^1, r_i^2, \dots, r_i^M\}$ represent the sets of selected trainable weights and corresponding ranks, constraint Eqn. (2b) refers to the range of the batch size for model training, and b_i is the batch size of the i -th edge server. The constraint Eqn. (2c) is used to pick up important weights in the transformer layer (see Section II-C). Eqn. (2d) guarantees that the rank of the m -th weight is selected in \mathcal{Q}^m where m ranges from 1 to $M = 4$ to represent different weights (i.e., $\mathbf{W}_q, \mathbf{W}_k, \mathbf{W}_v, \mathbf{W}_o$). Eqn. (2e) indicates the computing budget for the i -th edge server where $f_c(\cdot)$ maps the relationship between trainable weight structure to floating point operations per second (FLOPS) [56]. The optimization problem (2) is an MILP problem, which is typically NP-hard. Hence, we propose an automated federated pipeline framework to solve this problem from Section III-C to III-E.

C. Identification of important weights

Recalling in Fig. 5 (see Section II-C), when the whole training process is done, different weights have various average performances on the LoRA adapter. In practice, the situation is more complex, since different combinations of weights also result in various training performances. More importantly, under a computing budget, the i -th edge server needs to identify and predict the combinations of weights with LoRA adapters for the next round of training.

To identify a set of important weights for each edge server, FedPipe introduces an indicator for important weights to quantify the important level of parameters and the sensitivity of parameters in the training loss. The well-known principal components analysis (PCA) [57] algorithm identifies the most information-rich dimensions with larger singular values by employing matrix singular value decomposition (SVD). Motivated by this, we perform the SVD on $\mathbf{B}\mathbf{A}$ (see Section III-B) of each trainable weight before each round of the training.

Since larger singular values contain richer data information,

we characterize the importance of weights using the average singular value of each trainable weight. Additionally, we also devise a sensitivity-based importance scoring function based on sensitivity-based importance scoring [58]–[60]. Therefore, at the t -th training round, to properly measure the parameter contribution of the m -th trainable weight (LoRA adapter) for i -th edge server, the importance metric can be calculated as follows

$$s_i^{m,t} = \frac{1}{d_1} \sum_{j=1}^{d_1} \lambda_{i,j}^{m,t} + \phi(\mathbf{W}_i^{m,t}) \quad (3)$$

where $\lambda_{i,j}^{m,t}$ denotes the j -th singular value of the m -th trainable weight (LoRA adapter) for i -th edge server at the t -th training round, $\mathbf{W}_i^{m,t}$ represents the m -th trainable weight (LoRA adapter) for the i -th edge server at the t -th training round and d_1 is the total number of singular values. Here, $\phi(\cdot)$ is a sensitivity-based importance scoring function for model weights. To interpret $\phi(\cdot)$ function, we first define the magnitude of the gradient-weight product:

$$I(\mathbf{W}) = \frac{1}{d_2} \sum_{j=1}^{d_2} |w_j \nabla_{w_j} L(\mathbf{W})| \quad (4)$$

where w_j and $\nabla_{w_j} L(\mathbf{W})$ represent the j -th trainable parameter of the model parameter \mathbf{W} and its corresponding gradient, respectively. d_2 is the total number of model parameter \mathbf{W} .

Eqn. (4) essentially approximates the average change in loss per parameter when a parameter is zeroed out [58], [60]. However, the sensitivity in Eqn. (4) is not a reliable indicator of the importance of \mathbf{W} . This is because it is estimated based on one mini-batch data sample, where random sampling and complex training dynamics result in high variability and significant uncertainty in sensitivity estimation using Eqn. (4). Therefore, at the t -th training round, we address this problem by designing sensitivity smoothing and uncertainty quantification [59]:

$$\bar{I}^t(\mathbf{W}) = \lambda_1 \bar{I}^{t-1}(\mathbf{W}) + (1 - \lambda_1) I^t(\mathbf{W}) \quad (5)$$

$$\bar{U}^t(\mathbf{W}) = \lambda_2 \bar{U}^{t-1}(\mathbf{W}) + (1 - \lambda_2) |I^t(\mathbf{W}) - \bar{I}^t(\mathbf{W})| \quad (6)$$

where $0 < \lambda_1, \lambda_2 < 1$, $\bar{I}(\cdot)$ represents the smoothed sensitivity by exponential moving average, and $\bar{U}(\cdot)$ denotes the uncertainty term. Subsequently, the sensitivity-based importance scoring function $\phi(\cdot)$ is defined as the product of $\bar{I}(\cdot)$ and $\bar{U}(\cdot)$ [59]:

$$\phi^t(\mathbf{W}) = \bar{I}^t(\mathbf{W}) \bar{U}^t(\mathbf{W}) \quad (7)$$

As shown in Fig. 10, we observe that trainable weights with higher importance metrics exhibit better fine-tuning performance, i.e., lower PPL values, which further illustrates the effectiveness of the proposed importance metrics. With the importance of weights $s_i = \{s_i^m\}$, the i -th edge server can configure its set of LoRA adapters in the following section.

D. Heterogeneous LoRA Adapters Configuration

We propose an automatic configuration solution to select batch size and rank for each edge server, based on the proposed important weight indicators. Since exhaustive search for all

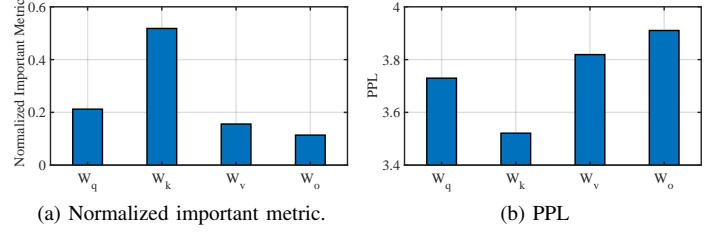


Fig. 10: The average normalized important metric and PPL of different trainable weights for GPT-2 models across 20 training rounds.

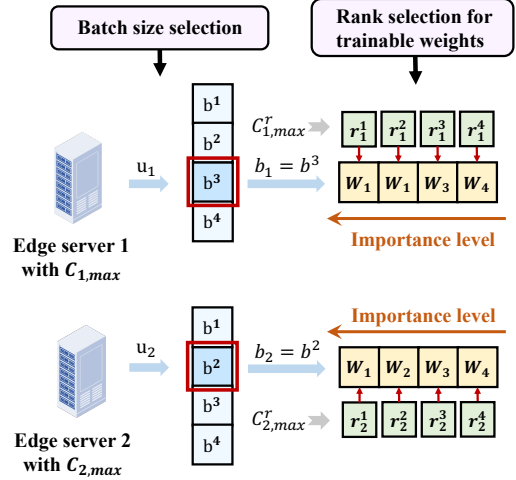


Fig. 11: The automated LoRA adapters configuration solution.

kinds of batch sizes, weights, and ranks is impossible due to the large search space, FedPipe leverages a two-stage search algorithm to tackle this problem as shown in Fig. 11. The first stage is to determine batch size, according to data diversity, and the second stage is to find the suitable rank under a computing budget.

To synchronize model aggregation across various edge servers (aligning the completion time for local model updates from different edge servers), the batch size selection is related to the computing capability at each edge server. For example, two edge servers with the computing capabilities of 20 TFLOPs and 40 TFLOPs, respectively, have different contributions to the LoRA adapters. Consequently, considering $\mathbf{C} = [C_{1,max}, C_{2,max}, \dots, C_{N,max}]$ computing capabilities of N edge servers, FedPipe calculates ratios of all values in \mathbf{C} , expressed as $\mathbf{U}_r = [u_1 : u_2 : \dots : u_N]$, and the batch sizes of edge servers are determined by $\mathbf{B} = \mathbf{U}_r \times b_{max}$. It is noted that any value $b_i < b_{min}$ in \mathbf{B} is replaced by b_{min} .

When the batch sizes \mathbf{B} is determined, for the i -th edge server, FedPipe can obtain its computing resource constraint only related to rank via $C_{i,max}^r = C_{i,max}/b_i$ based on Eqn. (2e). To pick up the ranks and weights from the sorted weights according to the importance (see Section III-C), FedPipe first starts from the most important weight, and then tries the rank value sequentially in \mathcal{Q}^m from high to low. If the computing capability corresponding to the highest ranked weight is below the maximum computing constraint $C_{i,max}^r$, it is selected. If not, the second-highest-ranked weight is used to

evaluate. The above steps repeat for the other weights until sets of weights and ranks reach the computing constraint $C_{i,\max}^r$. At the end, the rank adjustment is iterated for each weight, and the optimal LoRA adapters at each edge server are configured dynamically during every training round. We summarize the whole process steps in Algorithm 1.

Algorithm 1: FedPipe training.

Require: N is the total number of edge servers, \mathbf{U}_r is the ratio of computing budgets of N edge servers.
Data: $\{D_1, \dots, D_i, \dots, D_N\}$ where D_i is the local collected data on the i -th edge servers.

1 Server Executes:

2 initialize the global model $\mathbf{W}_g^{(0)}$ at $t = 0$;

3 $S \leftarrow \{C_1, \dots, C_N\}$;

4 $\mathbf{B} \leftarrow \max(b_{\min}, \mathbf{U}_r \times b_{\max})$;

5 **for** communication round t **do**

6 **for** edge server $C_i \in S$ **in parallel do**

7 $\mathbf{B}_i, \mathbf{A}_i \leftarrow \text{Auto Configuration}(i, b_i)$;

8 $\mathbf{W}_i^{t+1} \leftarrow \mathbf{W}_g^t + \mathbf{B}_i \mathbf{A}_i$;

9 $\mathbf{W}_i^{t+1} \leftarrow \text{Adam}(\mathbf{W}_i^{t+1}, b_i)$;

10 $\mathbf{W}_g^{t+1} \leftarrow \text{Model Aggregate}(\mathbf{W}_i^{t+1})$

11 Auto Configuration(i, b_i):

12 $C_{i,\max}^r \leftarrow C_{i,\max}/b_i$;

13 **for** $m = 1 : M$ **do**

14 $s_i^m \leftarrow \text{Weight Importance}(\mathbf{B}_i^m, \mathbf{A}_i^m)$;

15 $\text{index} \leftarrow \text{Sort_decent}(s_i)$;

16 **for** $m = \text{index}(1) : \text{index}(M)$ **do**

17 **for** $r = Q_{\max}^m : Q_{\min}^m$ **do**

18 $\mathcal{W}_i^m \leftarrow \mathbf{W}_i^m + \mathbf{B}_i^m \mathbf{A}_i^m$;

19 **if** $f_c(\mathcal{W}_i^m, r) \leq C_{i,\max}^r$ **then**

20 $\mathbf{B}_i^m, \mathbf{A}_i^m \leftarrow \text{set LoRA rank to } r$;

21 $C_{i,\max}^r \leftarrow C_{i,\max}^r - f_c(\mathcal{W}_i^m, r)$

22 **else**

23 **continue**;

24 **return** $\mathbf{B}_i, \mathbf{A}_i$;

E. Quantization for Adapters' Training

Apart from the LoRA adapter configuration, the limited and heterogeneous GPU memory resources of edge servers may also lead to an increase in the under-training rate, thus posing a significant challenge for LLM fine-tuning. Although model quantization has emerged as a promising solution to address memory constraints, existing methods do not consider varying quantization bits across edge servers.

Considering the heterogeneous GPU memory budgets of edge servers ($M_{i,\max}$, $i = 1, 2, \dots, N$), we quantize the pre-trained models with varying quantization bits, and only dequantize models for performing matrix multiplication with higher precision. Pre-trained models consume a significant amount of memory space, necessitating a high compression ratio to conserve memory (usually 4 bits or 8 bits). In contrast, LoRA adapter requires less memory space and is utilized for updates, hence a lower compression ratio (e.g., 16-bit floats (FP16)) is employed to maintain precision. Therefore, in FedPipe, we quantize pre-trained models with the maximum quantization bits based on memory budgets of edge servers, but keep LoRA adapters unchanged. In the following, we give details of our quantization.

In our design, we adopt the NormalFloat (NF) quantization built based on Quantile Quantization [61], which offers signifi-

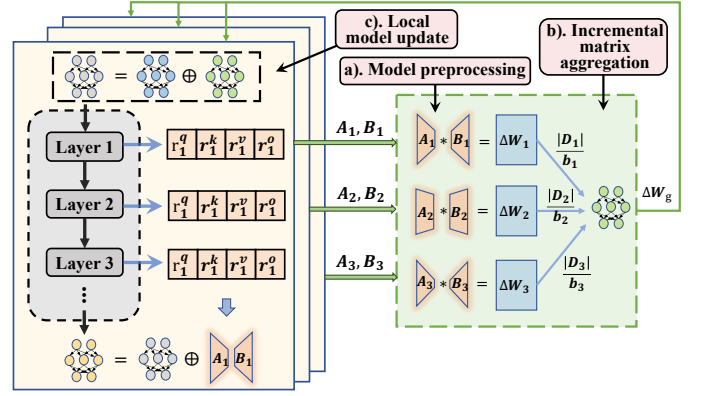


Fig. 12: Adapter aggregation of FedPipe framework.

cant benefits in model compression, computational complexity reduction, accuracy preservation, and hardware compatibility [62]. NF data type ensures that each quantization bin has an equal number of values for the input tensor. It estimates the quantile through the empirical cumulative distribution function, enhancing quantization accuracy.

Since pre-trained model weights usually follow a zero-mean normal distribution [62], we first transform all weights to a zero-mean normal distribution within $[-1, 1]$ range via standard deviation. After that, we estimate the $2^k + 1$ quantiles to obtain a k -bit quantile quantization data type and normalize the value of this data type into the $[-1, 1]$ range. Finally, we quantize an input weight tensor by normalizing it into $[-1, 1]$ range through absolute maximum rescaling. Once the weight range and data type range match, we estimate the 2^k values q_i of the data type as follows

$$q_i = \frac{1}{2} \left[Q \left(\frac{i}{2^k + 1} \right) + Q \left(\frac{i}{2^k + 1} \right) \right] \quad (8)$$

where $Q(\cdot)$ is the quantile function of the standard normal distribution. By this means, the pre-trained model quantization is done.

F. LoRA Adapters Aggregation and Deployment

Current FL model aggregation aggregates the whole models, but for LLM, transferring them to the central server brings a significant communication overhead (see Section II-B). Therefore, FedPipe only allows each edge server to transfer rank decomposition matrices \mathbf{B} and \mathbf{A} (see Section III-B) instead of the whole models in order to reduce the communication overhead. However, to merge all kinds of rank decomposition matrices from varying edge servers, we still face two challenges in aggregation and updating, respectively. On the one hand, the diverse rank decomposition matrices with different ranks from edge servers cannot be aggregated directly (e.g., different sizes of two edge servers' \mathbf{B} s cannot be added). On the other hand, even if the local models are aggregated, the central server recovers \mathbf{B} and \mathbf{A} for the edge server possibly leading to deterioration rather than improvement in the training performance. To combat above challenges, as illustrated in Fig. 12, the tailored heterogeneous model aggregation solution comprises the following three stages.

a) Model Preprocessing. Before aggregation, the central server achieves incremental matrices for participating edge servers. At the t -th training round, the incremental matrix of the m -th trainable weight (LoRA adapter) for i -th edge server is given by

$$\Delta \mathbf{W}_i^{m,t} = \mathbf{B}_i^{m,t} \cdot \mathbf{A}_i^{m,t} \quad (9)$$

where $\mathbf{B}_i^{m,t}$ and $\mathbf{A}_i^{m,t}$ denote the corresponding rank decomposition matrices.

b) Incremental Matrix Aggregation. At this stage, the central server aggregates the preprocessed incremental matrices from different edge servers, i.e.,

$$\Delta \mathbf{W}^{m,t} = \sum_{i=1}^N \frac{|D_i|/b_i}{\sum_{i=1}^N |D_i|/b_i} \Delta \mathbf{W}_i^{m,t} \quad (10)$$

c) Local Model Update. Instead of updating $\mathbf{B}_i^{m,t}$ and $\mathbf{A}_i^{m,t}$ directly, the i -th edge server updates $\Delta \mathbf{W}_i^{m,t}$ based on $\Delta \mathbf{W}^{m,t}$ dispatched by the central server. Moreover, recalling Section III-E, according to the memory constraint of the i -th edge server, the local model is quantized, and hence, $\Delta \mathbf{W}^{m,t}$ should be quantized for merging it into the local model. The updating policy is followed by

$$\mathbf{W}_i^{m,t+1} = \mathbf{W}_i^{m,t} + \text{quant}(\Delta \mathbf{W}_i^{m,t}), \quad (11)$$

$$\mathbf{B}_i^{m,t+1} = \bar{\mathbf{B}}_i^m, \mathbf{A}_i^{m,t+1} = \bar{\mathbf{A}}_i^m \quad (12)$$

where $\bar{\mathbf{A}}_i^m$ and $\bar{\mathbf{B}}_i^m$ are the reinitialized rank decomposition matrices, and $\text{quant}(\cdot)$ means the quantization function.

IV. IMPLEMENTATION AND EXPERIMENTAL SETUP

Models: We deploy two well-known LLMs, LLaMA2 [4] and GPT-2 [2]. The LLaMA2 model has been widely used for various natural language understanding tasks, including text generation, summarization, and questioning and answering. The GPT-2 is famous for its ability to generate coherent and relevant content, making it well suited for text generation tasks, such as text completion and language translation. The LLaMA2-7b model has 32 layers and 3.52 billion parameters, whereas the GPT-2 medium and large models have 24 layers and 355 million parameters and 36 layers and 774 million parameters, respectively.

Datasets and tasks: We evaluate the training performance of FedPipe for instruction-following (IF) tasks on Alpaca dataset [63] and natural language generation (NLG) tasks on E2E dataset [64]. The Alpaca dataset comprises approximately 52,000 samples which spans diverse domains such as philosophy, economics, sociology, and science, while the E2E dataset consists of around 42,000 training, 4,600 validation and 4,600 test examples from the restaurant domain. We fine-tune the LLaMA2-7B model on the Alpaca dataset for IF task, which outputs detailed and contextually relevant responses based on given instructions. Similarly, we train the GPT-2 model on the E2E dataset for NLG task, aiming to transform various forms of inputs into human-readable natural language.

Benchmarks: We compare FedPipe with three classical benchmarks: (1) **Vanilla Fine-Tuning (FT):** FT fine-tunes full parameters of LLMs on each edge server, which is the default fine-tuning technique in most NLP literature [44]. (2) **Low-**

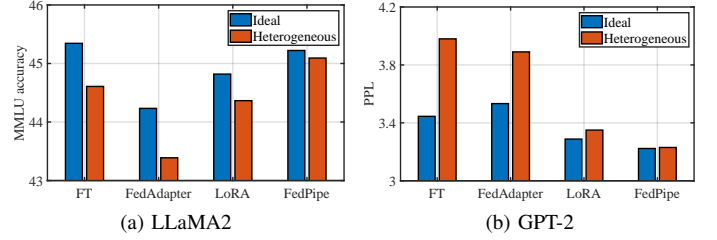


Fig. 13: The converged accuracy for LLaMA2-7b and GPT-2 models under heterogeneous and ideal settings.

Rank Adaptation (LoRA): LoRA introduces low-rank trainable modules [37] in parallel to weight matrices for LLM fine tuning. Training only low-rank trainable modules while freezing the rest of model parameters substantially reduces the number of trainable parameters without incurring additional inference latency. (3) **FedAdapter:** FedAdapter [43] is an edge-cutting FL framework tailored for efficient LLM fine-tuning. It identifies the optimal adapter configuration during the training process, catering to the demands of fine-tuning LLMs in a privacy-preserving manner while minimizing the training costs. To ensure fair comparisons, all benchmarks adopt the same model aggregation algorithm (FedAvg [53]) and random client sampling scheme, consistent with the default settings in prior FL literature [43], [65].

Hardware and hyper-parameters: We conduct experiments utilizing 16 NVIDIA GeForce RTX 3090-Ti GPU with the maximum memory of 24 GB. For resource heterogeneity, we constrain the each GPU's maximum memory available for model training by randomly selecting values from a uniform distribution between 12GB and 24GB. To ensure fair comparisons, we retain the consistent settings for FedPipe and benchmarks across different tasks. For IF task on the Alpaca dataset, mini-batch size, learning rate, and maximum sequence length are set to 2, 0.0001, and 384, respectively. Similarly, for the NLG task on the E2E dataset with GPT-2 medium, we set mini-batch size, learning rate, and maximum sequence length to 8, 0.0002, and 512, respectively. Considering the limited 24 GB memory of the NVIDIA GeForce RTX 3090-Ti, we reduce the mini-batch size to 4 while keeping other hyperparameters unchanged when training the GPT-2 large model. The number of selected participating edge servers is set to 15 and the rank is set to 4 by default unless specified otherwise. All edge servers run in synchronized mode [66].

V. EVALUATION

This section provides numerical results to evaluate the training performance of FedPipe framework and the effectiveness of each meticulously designed component.

A. Overall Performance Evaluation

Converged accuracy. Fig. 13 shows the comparison between FedPipe and the three other benchmarks in converged accuracy on LLaMA2 and GPT-2 models under heterogeneous and ideal settings. It is clear that the proposed FedPipe framework outperforms the other benchmarks in both settings. In the homogeneous setting, the FedPipe framework reaches

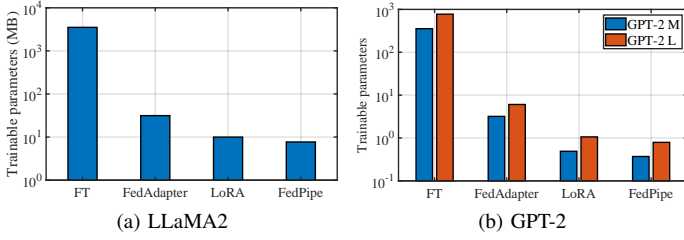


Fig. 14: The number of trainable parameters for LLaMA2-7b and GPT-2 models under heterogeneous setting, respectively.

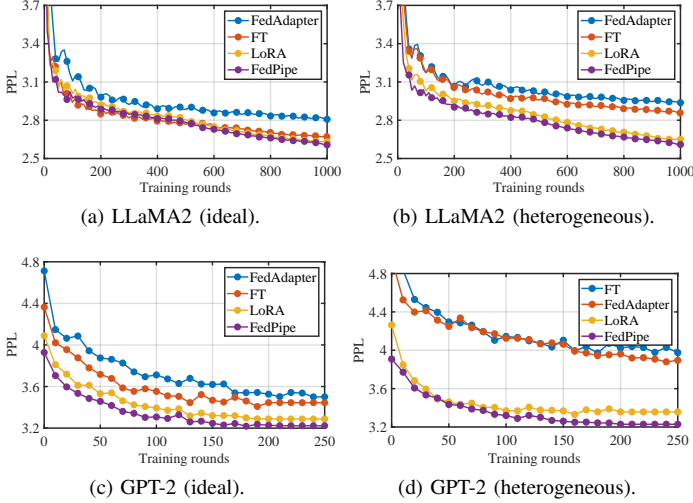


Fig. 15: The convergence rate for LLaMA2-7b and GPT-2 models under heterogeneous and ideal settings.

comparable accuracy on LLaMA2 model and outperforms the FT, FedAdapter, and LoRA benchmarks for PPL by 0.22, 0.31, and 0.06, respectively. This superiority is attributed to tailored important weights identification, which prioritizes the fine-tuning of key weights, thereby enhancing the efficiency of fine-tuning LLMs and achieving higher converged accuracy. Moreover, due to the lack of adaptive rank adjustment for computing heterogeneity, all benchmarks exhibit notably inferior converged accuracy under ideal than heterogeneous settings. In contrast, the FedPipe framework automatically adjusts rank size based on heterogeneous computing resources and only experiences a slight increase in PPL, nearly 0.01, under heterogeneous than ideal settings. Moreover, the performance gap between FedPipe and the other benchmarks is much larger than that in ideal settings, further demonstrating the superior adaptability of FedPipe to heterogeneous scenarios.

Trainable parameters. Fig. 14 presents the number of trainable parameters for deploying FedPipe and other benchmarks on LLaMA2 and GPT-2 models under heterogeneous and ideal settings. In the ideal setting, we observe that FedPipe framework and LoRA with fixed rank size exhibit identical number of trainable parameters. This is due to FedPipe’s capability in fine-tuning all four trainable weights and selecting the maximum rank for each weight without resource constraints. FedPipe has the fewest number of trainable parameters under heterogeneous setting, which is nearly 25% lower than that

under the ideal setting. Deploying FedPipe on LLaMA2 and GPT-2 models results in approximately 7.69M and 0.37M trainable parameters, whereas the trainable parameters for FT and FedAdapter framework is over 350 and 4 times larger than FedPipe on LLaMA2 model and about 960 and 8 times on GPT-2 models, respectively. The reduction in trainable parameters significantly diminishes the computing and communication overheads of fine-tuning LLMs, facilitating the deployment of LLMs. It is noteworthy that FedPipe does not require iterative searching for the optimal depth and width of the adapter layer, reducing the time overhead of the training process. In contrast, FedAdapter selects adapters from three different configuration groups, whereas FedPipe only adapts an initialized adapter configuration, and thus substantially saves storage resources compared to FedAdapter.

Convergence rate. Fig. 15 compares the convergence rate for FedPipe and the other three benchmarks under heterogeneous and ideal settings. In the ideal and heterogeneous setting, FedPipe exhibits the fastest convergence speed, outpacing FT, FedAdapter, and LoRA by factors of 6, 2.7, and 2 to achieve 3.6 PPL as well as 24, 18 and 2 to achieve 4.0 PPL on GPT-2 model, respectively. Moreover, FedPipe demonstrates comparable performance to FT, and is only lower by 0.23 on LLaMA2 model and even outperforms FT by 0.22 in the metric of PPL on GPT-2 model under ideal setting. This primarily stems from our design of the important layer identification strategy, which prioritizes the fine-tuning of crucial layers to reduce the under-training rate, thus expediting model training. Conversely, in the heterogeneous setting, FedPipe surpasses other benchmarks in convergence rate and accuracy due to its adaptive adjustment of LoRA’s rank size to accommodate the heterogeneous computing resources of clients. Due to the absence of heterogeneous LoRA adapter configuration, the convergence speed and accuracy of FT, FedAdapter, and LoRA rapidly deteriorate in heterogeneous settings. For the GPT-2 models, we also conducted a comprehensive comparison of the precision across various metrics under homogeneous and heterogeneous settings, which is summarized in Table II.

B. Ablation Evaluation

Important weights identification (IWI). Fig. 16a shows the impact of the selection of trainable weights on GPT2-L model under heterogeneous setting. Considering that the average number of trainable weights in our training process is approximately 3, we compare the IWI method with a random combination of three trainable weights for fair comparison. The proposed IWI method exhibits lower PPL than all three random combinations of weights, which demonstrates the effectiveness of our IWI method. This is because large singular values usually correspond to the primary directions of variation in model weights, reflecting where the density of principal information is high. Therefore, it is efficient to prioritize fine-tuning the trainable weights with large singular values. Additionally, training performance on other metrics is summarized in Table III.

Heterogeneous configuration (HC). Fig. 16b presents the impact of the selection of rank size on model training. We compare our proposed HC method with conventional LoRA

Model	Method	#Trainable Parameters	E2E NLG Challenge				
			BLEU	NIST	MET	ROUGE-L	CIDEr
GPT-2 M (Ideal)	FT	354.92M	68.2	8.62	46.2	71.0	2.47
	FedAdapter	3.19M	65.4	8.26	41.9	68.6	2.06
	LoRA	0.49M	69.1	8.74	46.3	70.6	2.46
	FedPipe	0.49M	69.6	8.79	46.9	70.6	2.44
GPT-2 M (Hetero)	FT	354.92M	60.5	8.12	41.0	64.4	1.92
	FedAdapter	3.19M	61.6	8.19	42.1	65.8	2.12
	LoRA	0.49M	68.4	8.65	46.1	70.3	2.45
	FedPipe	0.37M	69.4	8.77	46.9	70.9	2.43
GPT-2 L (Ideal)	FT	774.03M	68.5	8.78	46.0	69.9	2.45
	FedAdapter	6.05M	65.7	8.53	42.2	67.9	2.08
	LoRA	1.06M	68.9	8.69	46.4	70.8	2.44
	FedPipe	1.06M	69.8	8.82	46.8	70.7	2.51
GPT-2 L (Hetero)	FT	774.03M	60.2	8.10	40.8	64.1	2.01
	FedAdapter	6.05M	60.3	8.09	40.9	64.0	1.90
	LoRA	1.06M	67.9	8.57	45.9	70.4	2.43
	FedPipe	0.79M	69.6	8.80	46.3	70.6	2.49

TABLE II: GPT-2 medium (M) and large (L) with different adaptation methods on the E2E NLG Challenge.

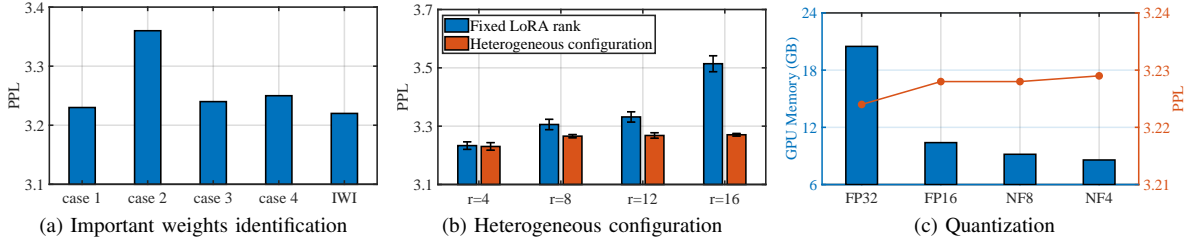


Fig. 16: Ablation Evaluation on GPT2-L model.

Weight Index	E2E NLG Challenge				
	BLEU	NIST	MET	ROUGE-L	CIDEr
$W_q + W_k + W_v$ (case 1)	69.1	8.70	46.7	70.4	2.44
$W_q + W_k + W_o$ (case 2)	68.1	8.76	45.3	68.9	2.39
$W_q + W_v + W_o$ (case 3)	69.2	8.72	46.6	70.5	2.43
$W_k + W_v + W_o$ (case 4)	69.4	8.73	46.7	70.4	2.43
IWI	69.6	8.80	46.3	70.6	2.49

TABLE III: GPT-2 large model with different combinations of trainable weights on the E2E NLG challenge.

schemes with different fixed rank sizes. It is observed that as the rank increases from 4 to 16, the PPL of the conventional LoRA framework grows rapidly from 3.23 to 3.51, nearly 9%, indicating an increasingly severe influence of the heterogeneous computing resource across clients on model training. This is attributed to the observation that the larger rank implies heavier computing workloads, leading to lower under-training rates. Conversely, the PPL of the HC method increases slightly with the rank, owing to our design of adaptively adjusting the rank based on heterogeneous computing capabilities. Moreover, the performance gap between HC method and LoRA with fixed rank sizes significantly widens with the increase in rank, further revealing the effectiveness of HC method. Similarly, the training performance on other metrics is shown in Table IV.

Quantization. Fig. 16c illustrates the GPU memory space and training accuracy under different quantization bits. The GPU memory space of FP32 is significantly larger than other quantization levels, 20.5 GB, where the model takes up 3.14 GB, which is approximately 1.9, 3.2, and 4.9 times that of FP16, NF8, and NF4, respectively. Quantization bit makes trade off between memory space and training accuracy

	Rank	E2E NLG Challenge				
		BLEU	NIST	MET	ROUGE-L	CIDEr
Fixed LoRA rank	$r = 8$	66.8	8.48	46.2	70.7	2.39
	$r = 12$	68.8	8.68	46.4	70.8	2.43
	$r = 16$	69.4	8.75	46.5	71.3	2.46
HC	$r_{max} = 8$	69.4	8.73	46.8	71.1	2.46
	$r_{max} = 12$	69.6	8.77	46.9	70.9	2.43
	$r_{max} = 16$	69.6	8.80	46.3	70.6	2.49

TABLE IV: GPT-2 large model with different heterogeneous configurations on the E2E NLG challenge.

Quantization	E2E NLG Challenge				
	BLEU	NIST	MET	ROUGE-L	CIDEr
FP32	70.1	8.83	46.5	71.7	2.50
FP16	69.6	8.79	46.2	70.6	2.49
NF8	69.5	8.75	46.8	71.0	2.44
NF4	69.4	8.77	46.9	70.9	2.43

TABLE V: FedPipe on GPT-2 large model with different quantization bits on the E2E NLG challenge.

of LLMs. It is observed that as the number of quantization bits diminishes, the training accuracy of the model only slightly decreases. FP32 achieves slightly higher training accuracy, i.e., with PPL 3.224, whereas FP16, NF8, and NF4 exhibit similar lower training accuracy, with PPL approximately 3.228. The proposed quantization scheme further reduces the memory requirements of the FedPipe framework, thereby improving its scalability. A more comprehensive comparison is illustrated in Table V.

VI. RELATED WORK

Parameter-efficient fine-tuning: PEFT has recently emerged as a promising approach for efficient LLM fine-

tuning, which strikes a balance between the number of trainable parameters and training accuracy in NLP tasks. Among various PEFT approaches, ADAPTER [35], [36], [38] and LoRA [37] stand out as the most attractive techniques for substantially reducing trainable parameters without compromising LLM fine-tuning performance. ADAPTER inserts small trainable modules into each transformer block while keeping the parameters of the pre-trained model frozen to improve training efficiency. Compacter [38] is a variant of ADAPTER that achieves lower parameter complexity based on shared information across adapters and low-rank subspaces of the model. However, the ADAPTER approaches introduce additional computing overhead in adapter layers, increasing the LLM fine-tuning latency, especially with smaller batch sizes. In contrast, LoRA [37] optimizes the variation of dense layers with low-rank decomposition matrices while keeping pre-trained model parameters frozen. Unlike ADAPTER, the low-rank matrices are inserted into the fine-tuned modules in a parallel manner, mitigating any additional training latency and thus enhancing the efficiency of LLM fine-tuning.

FL paradigm for LLMs: PEFT needs to fine-tune the LLMs based on domain-specific data of downstream tasks. However, clients may be reluctant to share raw data with the server due to data privacy concerns, especially privacy-sensitive data such as medical images. A promising solution to this issue is the FL paradigm, which enables multiple users to train models without sharing raw data. Recently, some research efforts have been made to merge LLM fine-tuning with the FL paradigm. [65] is the first work to integrate FL with LLM fine-tuning, comprehensively validating the effectiveness of the FedNLP framework on four common formulations of NLP tasks: text classification, sequence tagging, question answering, and seq2seq generation. FedAdapter [43] addresses the high training cost of FedNLP, which expedites the model convergence rate by progressively upgrading adapter configurations as well as continuously profiling future adapter configurations. However, existing works only focus on the traditional language models such as BART or BERT, whereas the most prevalent LLMs (e.g., GPT-2 [2]) with a significant number of parameters are ignored.

Model compression and quantization: The unprecedented number of parameters for LLMs renders computation and storage significant bottlenecks for LLM fine-tuning. Model compression and quantization have emerged as promising techniques to reduce model storage size and accelerate inference by decreasing bit precision [67], [68]. GPTQ [69] leverages second-order information for error compensation, significantly enhancing model accuracy and training efficiency. The authors of [70] propose an edge-cutting quantization method, named AWQ, to quantize weights into low-bit integers, thereby reducing the hardware barrier and speeding up token generation. Unlike previous work on quantization for LLM inference, SwitchBack layers [71] investigates backpropagation through quantized weights over 1B parameters and QLoRA [62] quantizes weights into 4-bit NormalFloat and backpropagates gradients into low-rank structure with the pre-trained LLMs.

Resource heterogeneity: The resource heterogeneity [29], [50], [72] poses a significant challenge to deploying FL frameworks [73]–[75] for LLMs. Clients with limited computing or memory resources require more time to complete local model updates, impeding the FL training process or even being excluded from model training. Although there are papers considering resource heterogeneity in general FL [76], there is no existing work that addresses resource heterogeneity in FL frameworks for LLM fine-tuning.

VII. CONCLUSION

In this paper, we have proposed and implemented FedPipe, an automated federated pipeline, to facilitate LLM FL fine-tuning in edge servers with heterogeneous computing resources. We have modeled the problem as a MILP to guide our design. To solve the problem, we have first selected important weights, and configured the corresponding parameters under computing budgets at edge servers for their LoRA adapters. We have also quantized LoRA adapters to further reduce memory space. Our extensive evaluations have demonstrated that FedPipe achieves significantly better performance than the state-of-the-art baselines in LLM FL.

REFERENCES

- [1] Z. Lin, G. Qu, Q. Chen, X. Chen, Z. Chen, and K. Huang, "Pushing large language models to the 6g edge: Vision, challenges, and opportunities," *arXiv preprint arXiv:2309.16739*, 2023.
- [2] A. Radford, J. Wu, R. Child, D. Luan, D. Amodei, I. Sutskever *et al.*, "Language Models are Unsupervised Multitask Learners," *OpenAI blog*, vol. 1, no. 8, p. 9, Feb. 2019.
- [3] T. Brown, B. Mann, N. Ryder, M. Subbiah, J. D. Kaplan, P. Dhariwal, A. Neelakantan, P. Shyam, G. Sastry, A. Askell *et al.*, "Language Models are Few-Shot Learners," Dec. 2020, pp. 1877–1901.
- [4] H. Touvron, T. Lavril, G. Izacard, Y. Martinet, M.-A. Lachaux, T. Lacroix, B. Rozière, N. Goyal, E. Hambro, F. Azhar *et al.*, "Llama: Open and Efficient Foundation Language Models," *arXiv preprint arXiv:2302.13971*, Feb. 2023.
- [5] A. Chowdhery, S. Narang, J. Devlin, M. Bosma, G. Mishra, A. Roberts, P. Barham, H. W. Chung, C. Sutton, S. Gehrmann *et al.*, "Palm: Scaling Language Modeling with Pathways," *Journal of Machine Learning Research*, vol. 24, no. 240, pp. 1–113, Aug. 2023.
- [6] L. Jiang, F. Svoboda, and N. D. Lane, "FDAPT: Federated Domain-adaptive Pre-training for Language Models," *arXiv preprint arXiv:2307.06933*, Nov. 2023.
- [7] Z. Lin, G. Qu, X. Chen, and K. Huang, "Split learning in 6g edge networks," *IEEE Wirel. Commun.*, 2024.
- [8] Y. Qiu, H. Chen, X. Dong, Z. Lin, I. Y. Liao, M. Tistarelli, and Z. Jin, "Ifvit: Interpretable fixed-length representation for fingerprint matching via vision transformer," *arXiv preprint arXiv:2404.08237*, 2024.
- [9] Z. Enghardt, C. Ma, M. E. Morris, X. Xu, C.-C. Chang, L. Qin, X. Liu, S. Patel, V. Iyer *et al.*, "From Classification to Clinical Insights: Towards Analyzing and Reasoning About Mobile and Behavioral Health Data With Large Language Models," *arXiv preprint arXiv:2311.13063*, Nov. 2023.
- [10] Z. Nan, H. Guan, X. Shen, and C. Liao, "Deep NLP-Based Co-evolution for Synthesizing Code Analysis from Natural Language," in *Proc. of the 30th CC*, Feb. 2021, pp. 141–152.
- [11] J. Peng, Z. Chen, Z. Lin, H. Yuan, Z. Fang, L. Bao, Z. Song, Y. Li, J. Ren, and Y. Gao, "Sums: Sniffing unknown multiband signals under low sampling rates," *arXiv preprint arXiv:2405.15705*, 2024.
- [12] Z. Fang, Z. Lin, S. Hu, H. Cao, Y. Deng, X. Chen, and Y. Fang, "Ic3m: In-car multimodal multi-object monitoring for abnormal status of both driver and passengers," *arXiv preprint arXiv:2410.02592*, 2024.
- [13] H. Yuan, Z. Chen, Z. Lin, J. Peng, Z. Fang, Y. Zhong, Z. Song, X. Wang, and Y. Gao, "Graph learning for multi-satellite based spectrum sensing," in *2023 IEEE 23rd International Conference on Communication Technology (ICCT)*, 2023, pp. 1112–1116.
- [14] Z. Lin, L. Wang, J. Ding, B. Tan, and S. Jin, "Channel power gain estimation for terahertz vehicle-to-infrastructure networks," *IEEE Commun. Lett.*, vol. 27, no. 1, pp. 155–159, 2022.

- [15] H. Yuan, Z. Chen, Z. Lin, J. Peng, Z. Fang, Y. Zhong, Z. Song, and Y. Gao, "Satsense: Multi-satellite collaborative framework for spectrum sensing," *arXiv preprint arXiv:2405.15542*, 2024.
- [16] Z. Lin, L. Wang, J. Ding, Y. Xu, and B. Tan, "Tracking and transmission design in terahertz v2i networks," *IEEE Transactions on Wireless Communications*, vol. 22, no. 6, pp. 3586–3598, 2022.
- [17] B. Yuan, Y. He, J. Davis, T. Zhang, T. Dao, B. Chen, P. S. Liang, C. Re, and C. Zhang, "Decentralized Training of Foundation Models in Heterogeneous Environments," Dec. 2022, pp. 25 464–25 477.
- [18] Z. Lin, G. Zhu, Y. Deng, X. Chen, Y. Gao, K. Huang, and Y. Fang, "Efficient parallel split learning over resource-constrained wireless edge networks," *IEEE Trans. Mob. Comput.*, 2024.
- [19] M. Hu, J. Zhang, X. Wang, S. Liu, and Z. Lin, "Accelerating federated learning with model segmentation for edge networks," *IEEE Transactions on Green Communications and Networking*, 2024.
- [20] Z. Lin, X. Hu, Y. Zhang, Z. Chen, Z. Fang, X. Chen, A. Li, P. Vepakomma, and Y. Gao, "Splitlora: A split parameter-efficient fine-tuning framework for large language models," *arXiv preprint arXiv:2407.00952*, 2024.
- [21] Z. Lin, G. Qu, W. Wei, X. Chen, and K. K. Leung, "Adaptsfl: Adaptive split federated learning in resource-constrained edge networks," *arXiv preprint arXiv:2403.13101*, 2024.
- [22] A. Karagyris, R. Umerton, M. J. Sheller, A. Aristizabal, J. George, A. Wuest, S. Pati, H. Kassem, M. Zenk, U. Baid *et al.*, "Federated Benchmarking of Medical Artificial Intelligence with MedPerf," *Nature Machine Intelligence*, vol. 5, no. 7, pp. 799–810, Jul. 2023.
- [23] Y. Zhang, Z. Lin, Z. Chen, Z. Fang, W. Zhu, X. Chen, J. Zhao, and Y. Gao, "Sattfed: A resource-efficient leo satellite-assisted heterogeneous federated learning framework," *arXiv preprint arXiv:2409.13503*, 2024.
- [24] J. Shin, Y. Li, Y. Liu, and S.-J. Lee, "FedBalancer: Data and Pace Control for Efficient Federated Learning on Heterogeneous Clients," in *Proc. of the 20th MobiSys*, Jun. 2022, pp. 436–449.
- [25] K. Panchal, S. Choudhary, N. Parikh, L. Zhang, and H. Guan, "Flow: Per-instance Personalized Federated Learning," *Proc. of the 37th NeurIPS*, Dec. 2023.
- [26] Y. Zhang, H. Chen, Z. Lin, Z. Chen, and J. Zhao, "Fedac: A adaptive clustered federated learning framework for heterogeneous data," *arXiv preprint arXiv:2403.16460*, 2024.
- [27] X. Shuai, Y. Shen, S. Jiang, Z. Zhao, Z. Yan, and G. Xing, "BalanceFL: Addressing Class Imbalance in Long-Tail Federated Learning," in *21st ACM/IEEE IPSN*, May. 2022, pp. 271–284.
- [28] S. Dai, B. Y. Chen, J. yong Sohn, S. M. I. Alam, R. Balakrishnan, S. Banerjee, N. Himayat, and K. Lee, "FedGP: Buffer-based Gradient Projection for Continual Federated Learning," in *Proc. of the 6th MLSys*, May 2023.
- [29] Z. Lin, Z. Chen, Z. Fang, X. Chen, X. Wang, and Y. Gao, "FedSN: A Federated Learning Framework over Heterogeneous LEO Satellite Networks," *IEEE Trans. Mob. Comput.*, Nov. 2023.
- [30] I. Panopoulos, S. Nikolaidis, S. I. Venieris, and I. S. Venieris, "Exploring the Performance and Efficiency of Transformer Models for NLP on Mobile Devices," in *28th ISCC*, Jul. 2023, pp. 1–4.
- [31] D. Cai, S. Wang, Y. Wu, F. X. Lin, and M. Xu, "Federated Few-Shot Learning for Mobile NLP," in *Proceedings of the 29th MobiCom*, Oct. 2023, pp. 1–17.
- [32] Y. Chen, Y. Yan, Q. Yang, Y. Shu, S. He, and J. Chen, "Confidant: Customizing Transformer-based LLMs via Collaborative Edge Training," *arXiv preprint arXiv:2311.13381*, Nov. 2023.
- [33] X. Ouyang, Z. Xie, H. Fu, S. Cheng, L. Pan, N. Ling, G. Xing, J. Zhou, and J. Huang, "Harmony: Heterogeneous Multi-Modal Federated Learning through Disentangled Model Training," in *Proc. of the 21st MobiSys*, Jun. 2023, pp. 530–543.
- [34] X. Ouyang, S. M. A. Ansari, F. X. Lin, and Y. Ji, "Efficient NLP Model Finetuning via Multistage Data Filtering," in *Proc. of the 32nd IJCAI*, Aug. 2023, pp. 4091–4099.
- [35] N. Houlsby, A. Giurugi, S. Jastrzebski, B. Morrone, Q. De Laroussilhe, A. Gesmundo, M. Attariyan, and S. Gelly, "Parameter-Efficient Transfer Learning for NLP," in *Proc. of the 36th ICML*, Jun. 2019, pp. 2790–2799.
- [36] J. Pfeiffer, A. Kamath, A. Rücklé, K. Cho, and I. Gurevych, "Adapter-Fusion: Non-Destructive Task Composition for Transfer Learning," in *Proc. of the 16th EACL*, Apr. 2021, pp. 487–503.
- [37] E. J. Hu, Y. Shen, P. Wallis, Z. Allen-Zhu, Y. Li, S. Wang, L. Wang, and W. Chen, "LoRA: Low-Rank Adaptation of Large Language Models," in *Proc. of the 10th ICLR*, Jan. 2022.
- [38] R. Karimi Mahabadi, J. Henderson, and S. Ruder, "Compacter: Efficient Low-Rank Hypercomplex Adapter Layers," Dec. 2021, pp. 1022–1035.
- [39] Y.-L. Sung, V. Nair, and C. A. Raffel, "Training Neural Networks with Fixed Sparse Masks," Dec. 2021, pp. 24 193–24 205.
- [40] T. Zhang, T. Feng, S. Alam, M. Zhang, S. S. Narayanan, and S. Avestimehr, "Gpt-fl: Generative pre-trained model-assisted federated learning," *arXiv preprint arXiv:2306.02210*, Sep. 2023.
- [41] Z. Hu, L. Wang, Y. Lan, W. Xu, E.-P. Lim, L. Bing, X. Xu, S. Poria, and R. Lee, "LLM-Adapters: An Adapter Family for Parameter-Efficient Fine-Tuning of Large Language Models," in *Proc. of the 28th EMNLP*, Dec. 2023, pp. 5254–5276.
- [42] Y. Sheng, S. Cao, D. Li, C. Hooper, N. Lee, S. Yang, C. Chou, B. Zhu, L. Zheng, K. Keutzer *et al.*, "S-LoRA: Serving Thousands of Concurrent LoRA Adapters," *arXiv preprint arXiv:2311.03285*, Nov. 2023.
- [43] D. Cai, Y. Wu, S. Wang, F. X. Lin, and M. Xu, "Efficient Federated Learning for Modern NLP," in *Proc. of the 29th MobiCom*, Oct. 2023, pp. 1–16.
- [44] J. D. M.-W. C. Kenton and L. K. Toutanova, "BERT: Pre-Training of Deep Bidirectional Transformers for Language Understanding," in *Proc. of 17th NAACL-HLT*, Jun. 2019, pp. 4171–4186.
- [45] X. Liu, T. Pang, and C. Fan, "Federated prompting and chain-of-thought reasoning for improving llms answering," in *The 16th KSEM*, Aug. 2023, pp. 3–11.
- [46] T. Che, J. Liu, Y. Zhou, J. Ren, J. Zhou, V. Sheng, H. Dai, and D. Dou, "Federated Learning of Large Language Models with Parameter-Efficient Prompt Tuning and Adaptive Optimization," in *Proc. of the 28th EMNLP*, Dec. 2023, pp. 7871–7888.
- [47] A. Reiszadeh, I. Tziotis, H. Hassani, A. Mokhtari, and R. Pedarsani, "Straggler-Resilient Federated Learning: Leveraging the Interplay Between Statistical Accuracy and System Heterogeneity," *IEEE Journal on Selected Areas in Information Theory*, vol. 3, no. 2, pp. 197–205, Jun. 2022.
- [48] W. Wu, L. He, W. Lin, R. Mao, C. Maple, and S. Jarvis, "SAFA: A Semi-Asynchronous Protocol for Fast Federated Learning With Low Overhead," *IEEE Transactions on Computers*, vol. 70, no. 5, pp. 655–668, May 2021.
- [49] T. Zhang, L. Gao, S. Lee, M. Zhang, and S. Avestimehr, "TimelyFL: Heterogeneity-aware Asynchronous Federated Learning with Adaptive Partial Training," in *2023 IEEE/CVF Conference on CVPR*, 2023, pp. 5063–5072.
- [50] S. Horvath, S. Laskaridis, M. Almeida, I. Leontiadis, S. Venieris, and N. Lane, "FJORD: Fair and Accurate Federated Learning under heterogeneous targets with Ordered Dropout," *Proc. of the 35th NeurIPS*, pp. 12 876–12 889, Dec. 2021.
- [51] X. Ouyang, Z. Xie, J. Zhou, G. Xing, and J. Huang, "ClusterFL: A Clustering-based Federated Learning System for Human Activity Recognition," *ACM Transactions on Sensor Networks*, vol. 19, no. 1, pp. 1–32, Dec. 2022.
- [52] S. Lyu, Z. Lin, G. Qu, X. Chen, X. Huang, and P. Li, "Optimal resource allocation for u-shaped parallel split learning," in *Proc. Globecom Wkshps*, 2023, pp. 197–202.
- [53] B. McMahan, E. Moore, D. Ramage, S. Hampson, and B. A. y Arcas, "Communication-Efficient Learning of Deep Networks from Decentralized Data," in *Proc. of the 20th ICAIS*, Apr. 2017, pp. 1273–1282.
- [54] S. Li, H. Lu, T. Wu, M. Yu, Q. Weng, X. Chen, Y. Shan, B. Yuan, and W. Wang, "Caraserve: Cpu-assisted and rank-aware lora serving for generative llm inference," *arXiv preprint arXiv:2401.11240*, 2024.
- [55] A. Aghajanyan, S. Gupta, and L. Zettlemoyer, "Intrinsic Dimensionality Explains the Effectiveness of Language Model Fine-Tuning," in *Proc. of 11th ACL-IJCNLP*, Aug. 2021, pp. 7319–7328.
- [56] J. Kaplan, S. McCandlish, T. Henighan, T. B. Brown, B. Chess, R. Child, S. Gray, A. Radford, J. Wu, and D. Amodei, "Scaling Laws for Neural Language Models," *arXiv preprint arXiv:2001.08361*, Jan. 2020.
- [57] C. Labrín and F. Urdinez, "Principal Component Analysis," in *R for political data science*, Nov. 2020, pp. 375–393.
- [58] P. Molchanov, A. Mallya, S. Tyree, I. Frosio, and J. Kautz, "Importance Estimation for Neural Network Pruning," in *2019 IEEE/CVF Conference on CVPR*, Jun. 2019, pp. 11 264–11 272.
- [59] Q. Zhang, S. Zuo, C. Liang, A. Bukharin, P. He, W. Chen, and T. Zhao, "PLATON: Pruning Large Transformer Models with Upper Confidence Bound of Weight Importance," in *Proc. of the 39th ICML*, Jul. 2022, pp. 26 809–26 823.
- [60] C. Liang, S. Zuo, M. Chen, H. Jiang, X. Liu, P. He, T. Zhao, and W. Chen, "Super Tickets in Pre-Trained Language Models: From Model Compression to Improving Generalization," in *Proc. of the 11th ACL-IJCNLP*, Aug. 2021, pp. 6524–6538.
- [61] T. Dettmers, M. Lewis, S. Shleifer, and L. Zettlemoyer, "8-bit Optimizers via Block-wise Quantization," Jan. 2022.

- [62] T. Dettmers, A. Pagnoni, A. Holtzman, and L. Zettlemoyer, “QLoRA: Efficient Finetuning of Quantized LLMs,” Dec. 2023.
- [63] (2023) “Stanford alpaca: An instruction-following llama model”. Available: https://github.com/tatsu-lab/stanford_alpaca.
- [64] J. Novikova, O. Dušek, and V. Rieser, “The E2E Dataset: New Challenges For End-to-End Generation,” in *Proc. of the 18th SIGDIAL*, Aug. 2017, pp. 201–206.
- [65] B. Y. Lin, C. He, Z. Ze, H. Wang, Y. Hua, C. Dupuy, R. Gupta, M. Soltanolkotabi, X. Ren, and S. Avestimehr, “FedNLP: Benchmarking Federated Learning Methods for Natural Language Processing Tasks,” in *Findings of the Association for Computational Linguistics: NAACL 2022*, Jul. 2022, pp. 157–175.
- [66] Q. Ho, J. Cipar, H. Cui, J. K. Kim, S. Lee, P. B. Gibbons, G. A. Gibson, G. R. Ganger, and E. P. Xing, “More Effective Distributed ML via a Stale Synchronous Parallel Parameter Server,” in *Proc. of the 27th NIPS*, Dec. 2013, pp. 1223–1231.
- [67] J. Bernstein, Y.-X. Wang, K. Azizzadenesheli, and A. Anandkumar, “signSGD: Compressed Optimisation for Non-Convex Problems,” in *Proc. of the 35th ICML*, Jul. 2018, pp. 560–569.
- [68] J. Wu, W. Huang, J. Huang, and T. Zhang, “Error Compensated Quantized SGD and its Applications to Large-scale Distributed Optimization,” in *Proc. of the 35th ICML*, Jul. 2018, pp. 5325–5333.
- [69] E. Frantar, S. Ashkboos, T. Hoefer, and D. Alistarh, “GPTQ: Accurate Post-Training Quantization for Generative Pre-trained Transformers,” in *Proc. of the 11th ICLR*, May 2023.
- [70] J. Lin, J. Tang, H. Tang, S. Yang, X. Dang, and S. Han, “Awq: Activation-aware weight quantization for llm compression and acceleration,” *arXiv preprint arXiv:2306.00978*, 2023.
- [71] M. Wortsman, T. Dettmers, L. Zettlemoyer, A. Morcos, A. Farhadi, and L. Schmidt, “Stable and Low-precision Training for Large-Scale Vision-Language Models,” Dec. 2023.
- [72] C. Li, X. Zeng, M. Zhang, and Z. Cao, “PyramidFL: A Fine-grained Client Selection Framework for Efficient Federated Learning,” in *Proc. of the 28th MobiCom*, Oct. 2022, pp. 158–171.
- [73] S. Wang, M. Lee, S. Hosseinalipour, R. Morabito, M. Chiang, and C. G. Brinton, “Device Sampling for Heterogeneous Federated Learning: Theory, Algorithms, and Implementation,” in *IEEE INFOCOM 2021-IEEE Conference on Computer Communications*, May 2021, pp. 1–10.
- [74] N. H. Tran, W. Bao, A. Zomaya, M. N. Nguyen, and C. S. Hong, “Federated Learning over Wireless Networks: Optimization Model Design and Analysis,” in *IEEE INFOCOM 2019-IEEE conference on computer communications*, Apr. 2019, pp. 1387–1395.
- [75] W. Wang, Y. Sun, B. Eriksson, W. Wang, and V. Aggarwal, “Wide Compression: Tensor Ring Nets,” in *2018 IEEE/CVF Conference on CVPR*, Jun. 2018, pp. 9329–9338.
- [76] G. Zhu, Y. Deng, X. Chen, H. Zhang, Y. Fang, and T. F. Wong, “Esfl: Efficient split federated learning over resource-constrained heterogeneous wireless devices,” *IEEE Internet of Things Journal*, 2024.